Commun. Comput. Chem
doi: 10.4208/cicc.2017.v5.n2.3

Vol.5, No.2, pp.46-62
June 2017

REGULAR ARTICLE

A Density Functional Theory Study of the Hydrolysis Mechanism of Sulfachloropyridazine

Yali Liu, Zhijun Shi, Qing Zhang, Mingliang Wang*

College of Chemistry and Environmental Engineering, Shenzhen University, Guangdong 518060, P. R. China

Received 26 April 2017; Accepted (in revised version) 10 June 2017

Abstract: Sulfonamide antibiotics are an important class of organic pollutant in the aquatic environments. To understand the hydrolysis behavior of sulfonamides, the hydrolysis mechanisms of a typical sulfonamide sulfachloropyridazine (SCP) were investigated using the density functional theory (DFT) at the B3LYP/6-31+G (d, p) level. SCP hydrolysis resembles nucleophilic substitution by water molecule attacking sulfonyl group (pathway 1) and heterocyclic aromatic ring (pathway 2) respectively. Due to the electrophilic center sulfur atom in pathway 1 carrying much larger positive charge than the carbon atom in the pathway 2, the sulfonyl group can be easily attacked by water molecule, and thus the pathway 1 can be dominant. By comparing the hydrolysis energy barrier of different forms of SCP, it was found that the SCP hydrolysis in neutral and once-protonated state are much more energetically favorable to proceed than the double protonated form. In addition, the hydrolysis path is not found for the dissociated anionic SCP. As the pH values in solution decreases, the corresponding neutral and once-protonated SCP increases, then the hydrolysis rate becomes faster, which is consistent with the experimental observations that the hydrolytic degradation rate at pH=4 is much faster than those of pH=7 and 9.

AMS subject classifications: 92E10, 80A30,

Key words: Hydrolysis Mechanism, Sulfonamides, Sulfachloropyridazine, the Density Functional Theory (DFT)

* Corresponding author. *E-mail*: wangml@szu.edu.cn

1 Introduction

Sulfonamides (SAs) are a group of synthetic antimicrobial agents [1](e.g., sulfachloropyridazine, sulfathiazole, sulfadiazine and sulfapyridine) which have been widely used in healthcare and veterinary antibiotics for decades [2,3]. All the sulfonamides, apart from sulfaguanidine, are compounds containing two basic and one acidic functional group [4]. The basic functional groups are the amine group of aniline and the heterocyclic base, and the acidic functional group is the sulfonamide group. The mechanism action of SAs is to inhibit the conversion of *p*-aminobenzoic acid and interrupt bacterial utilization of the compound in the synthesis of folic acid and ultimately of protein, purine and DNA [2,5]. Due to the low cost and broad spectrum of activity in preventing or treating bacterial infections and the effectiveness of growth promotion, SAs are extensively prescribed today as the popularly used antibiotic drugs or growth promoter with the increasing need of pharmaceuticals and veterinary medicine [6].

As SAs are persistent and non-biodegradable, the contamination of environment has recently raised concern in aquatic environments [7]. Although the SAs concentrations in the environmental samples are quite low ($ng \cdot L^{-1}$-$\mu g \cdot L^{-1}$), its high biological activity could cause significant changes in biosphere [2,6,8]. Thus, it is very important to understand the possible degradation ways of SAs for helping evaluate their environmental fate or the treatment of these kinds of substance. Many experimental studies reported that SAs are resistant to natural biodegradation, but they undergo abiotic degradation such as hydrolysis and photolysis. Like most of other organic substances [9], SAs may experience photolysis degradation with the presence of catalysts like TiO_2, Fe(III) or H_2O_2 in water solutions under the illumination of UV radiation[10]. Recently, the photolysis mechanisms of sulfachloropyridazine (SCP) and Sulfadiazine (SDZ) have been well investigated using quantum chemical approach [11,12]. Furthermore, as one of the most common reactions controlling abiotic degradation, hydrolysis is an important degradation path for most organic pollutants in the environment. Recently, Kumirska et al made a detailed experimental investigation on the hydrolysis of sulfonamides in aqueous solutions [4], the results indicate that SA hydrolysis was closely depending on the temperature and pH values. At 70°C, the hydrolytic degradation rate for SCP at pH=4 is much higher than those of pH=7 and 9. Two independent hydrolysis paths of SCP were proposed by Kumirska as shown in **Scheme 1**[4]. In the case of path 1, the nucleophilic substitution takes place in the sulfonyl group with sulphanilic acid and the corresponding heterocyclic base as the main products. In path 2, the nucleophilic aromatic substitution occurs in the heterocyclic aromatic ring with sulfanilamide as the primary product.

Although many experimental studies about the hydrolysis of SAs were carried out [4,13], the theoretical investigation on the mechanism of SAs hydrolysis has not been reported. In-depth understanding the hydrolysis mechanism of SAs will be highly beneficial for rational design of easily degradable novel sulfonamides. To confirm the sulfonamide hydrolysis mechanisms, the theoretical calculations were carried out for the hydrolysis process of SAs. In this study, taking the widely used antibiotic sulfachloropyridazine as a typical example, the different hydrolysis mechanisms were evaluated by using the density functional theory (DFT) at the level of 6-31+G (d, p) including conductor-like polarizable continuum solvation model [14].

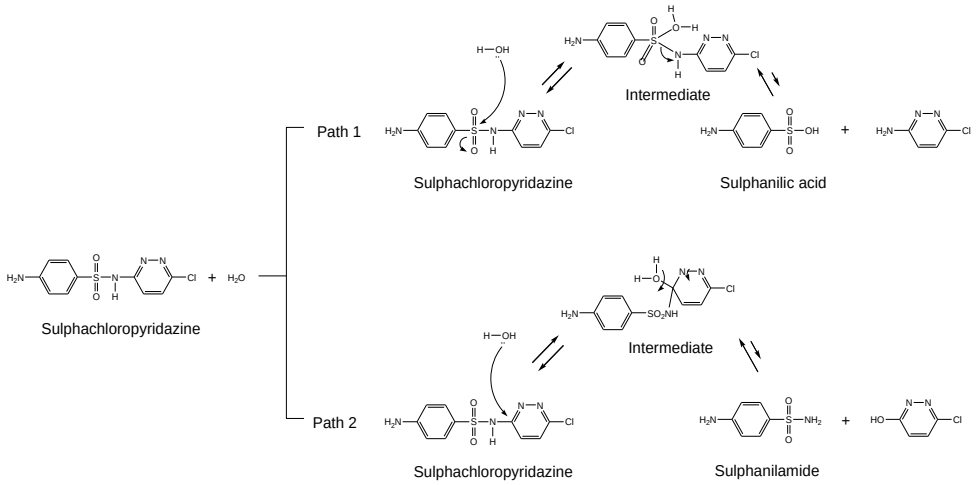

Scheme 1: Two proposed hydrolysis mechanisms of sulfachloropyridazine [4].

2 Method of Calculation

All the electronic calculations were performed with the Gaussian 09 suite of program using the density functional theory. DFT and time-dependent DFT have been widely used to study the molecular structure, bind energy and reaction mechanism due to its low cost and high accuracy [15-21]. Among the many implementations of DFT procedures, Becke's three-parameter expression with the correlation functional of Lee, Yang, and Parr (B3LYP) including non-linear components is widely used in most areas of quantum chemistry as of its high accuracy [22-24]. In the study of reaction mechanism, the standard 6-31+G (d,p) and 6-311++G(d, p) are frequently used [25-28]. In the early DFT study of the hydrolysis of Toluene-2,4-diisocyanate, it is illustrated that the energy barriers obtained from B3LYP/6-31+G(d, p) are very close to those of B3LYP/6-311++G(d, p) and CBS-QB3 [28]. Therefore, the B3LYP with 6-31+G (d, p) basis set was chosen in all the following calculations. As the hydrolysis of Sulfonamides occurs in aqueous solution, the reactive water molecule is

considered implicitly and the bulk water solvent effects are implicitly described by self-consistent reaction field (SCRF) method based on the conductor-like polarizable continuum model (CPCM) [29,30]. The geometries of all the reactants, products, transition states and intermediates are fully optimized. Based on the optimized geometries, the frequency analysis was performed to verify the characters of the transition states with only one imaginary frequency and stationary points without imaginary frequency [31-33]. In addition, the intrinsic reaction coordinate (IRC) calculations were performed to verify the reaction pathways correctly connecting reactants and products through the located transition states of the proposed mechanism [34,35]. Finally, the reactant or product complexes were obtained by applying the unconstrained optimization on the endpoints of IRC respectively [26-28,36]. The natural bond orbital (NBO) analysis was carried out to study the atomic charge distribution over the entire molecule [37,38].

3 Results and Discussion

The sulfachloropyridazine contains two basic and one acidic functional group. The basic functional groups are the amine group of aniline and the heterocyclic base, and the acidic functional group is the sulfonamide group, which is known to lose its proton relatively easily with its pK_a=5.5 [4,5]. The structure of sulfachloropyridazine can be characterized by pK_{a1} pK_{a2} and pK_{a3} values corresponding to the double protonated, once protonated and neutral forms [4]. **Figure 1** shows the possible forms of SCP at different pH values. The principle species depend on the pH of solution and pK_a values. Owing to the very low pK_{a1}(<2) resulted from heterocyclic base, SCP can exist in the double protonated form SCP (I) under very acidic conditions. The pK_{a2}=2.2 is caused by the aniline amino group of SCP[4,5], the once-protonated form SCP (II) dominates at pH<2.2. Due to the pK_{a3}=5.5 of sulfonamide group, sulfachloropyridazine is one typical weak acid. At pH≈(pK_{a2}+pK_{a3})/2=3.85, the

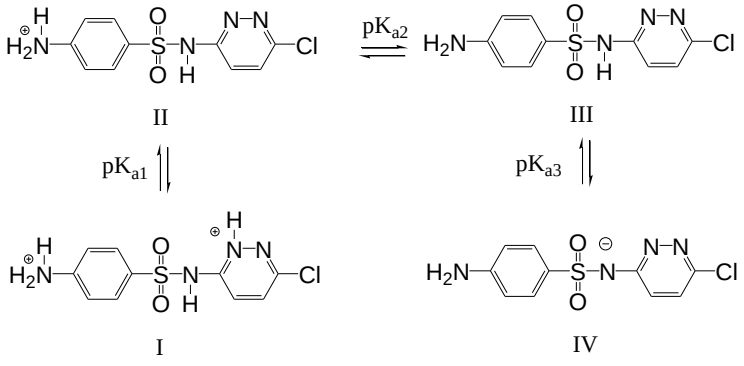

Figure 1: Forms of sulfachloropyridazine observed at different pH values[4].

neutral SCP (III) is predominant in solution. If the pH is higher than pK_{a3}=5.5, the SCP mainly exists in anionic form SCP (IV). In this case, the nucleophilic water molecule can be strongly repelled by the anionic SCP, the hydrolysis may not take place and the transition state in deed was not found by density functional theory. Therefore, only the neutral, once-protonated and double protonated SCP hydrolysis were presented in the context. **Figure 2** presents the optimized geometries of water molecule and SCP in three forms. As shown in **Figure 2**, the calculated NBO charges indicate that the sulfur atom and C1 carbon atom in the heterocyclic aromatic ring carry large positive charges acting as an electrophile. However, the oxygen of water molecule holds much negative charge (-1.035) acting as a nucleophile, which can attack on the electrophilic center of SCP in the hydrolysis. The optimized neutral SCP forms a distorted V configuration between pyridazine ring and benzene plane, which is in a good agreement with the experimental X-ray molecular crystal structure [39], the differences between the calculated bond lengths and the experimental data are less than 0.08 Å. It indicates that the B3LYP/6-31+G (d, p) level of theory is a reliable method to examine the hydrolysis mechanism of SCP. The total energies including zero-point energy (ZPE) of SCP in three different forms and water molecule are summarized in **Table 1**, which is required to estimate the relative energies of the hydrolysis.

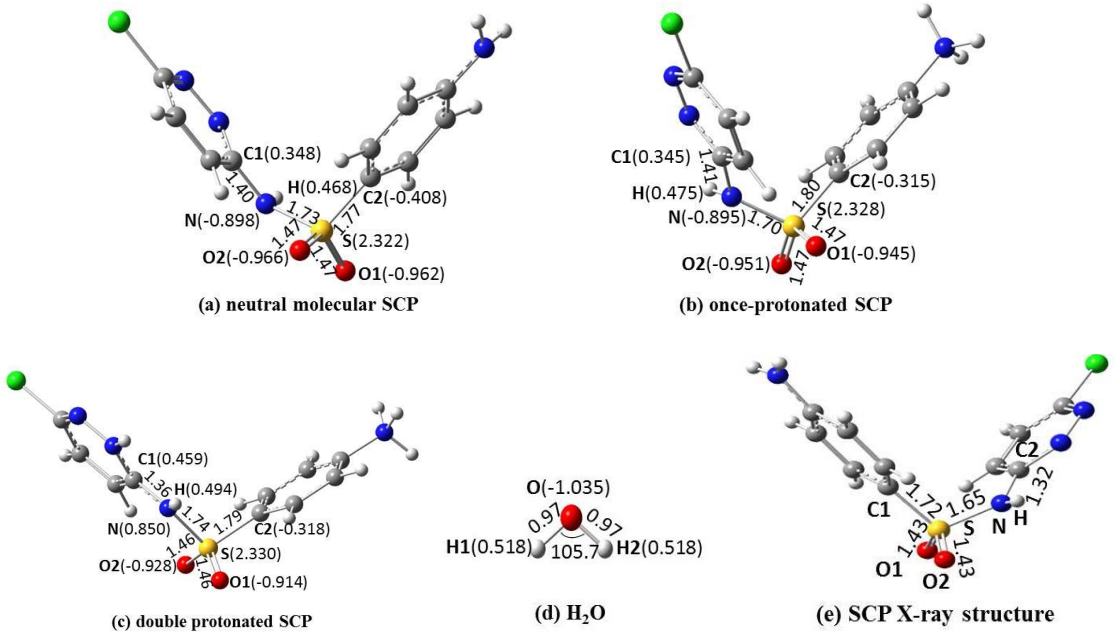

Figure 2: Optimized structures of sulfachloropyridazine in neutral form (a), once-protonated (b), double protonated (c) and water molecule (d), X-ray structure (e) [39]. The data with no brackets stands for bond lengths (Å); the data within brackets stands for NBO atomic charge (e).

Table 1. Total Energies including ZPE of SCP in three different forms and water

Compounds	Energies (Hartree)	ZPE (Hartree)	Total Energies with ZPE (Hartree)
Neutral molecular SCP (a)	-1614.294182	0.190471	-1614.103711
Once-prodonated SCP (b)	-1614.717011	0.205673	-1614.511338
Double protonated SCP (c)	-1615.141559	0.219900	-1614.921659
H_2O (d)	-76.442352	0.021197	-76.421155

3.1 Hydrolysis mechanisms of neutral molecular SCP

With the pH of solution between pK_{a2}=2.2 and pK_{a3}=5.5, the sulfachloropyridazine exists primarily in neutral form SCP (III) as shown in Fig. 1. Two possible hydrolysis pathways were proposed for neutral SCP in solution. In pathway 1, the nucleophilic substitution takes place by water molecule attacking the electrophile sulfonyl group; the sulfanilic acid and the corresponding heterocyclic base 3-Amino-6-chloropyridazine are the products of the SCP hydrolysis as illustrated in **Scheme 1**. In such a process, the stable intermediate **1** (**Figure 3**) was first obtained by forming a hydrogen bond O1-H…O2(1.93Å) between SCP and water

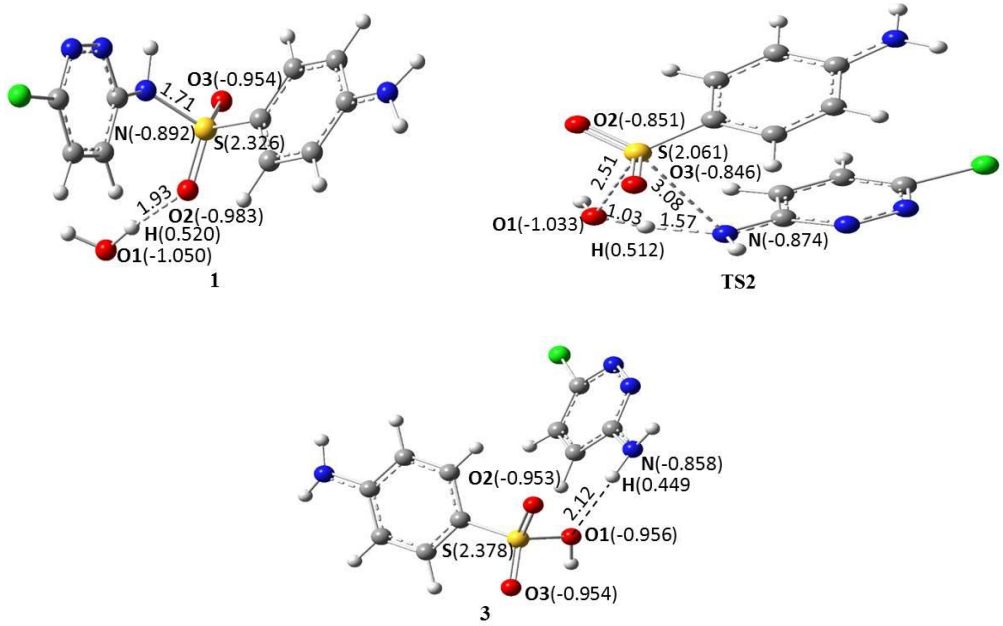

Figure 3: Optimized structures of intermediate **1**, transition state **TS2** and product **3** for the pathway 1 of neutral SCP hydrolysis mechanism.

molecule, which leads to the total energy of the intermediate **1** slightly lowered by 1.59 kcal·mol^{-1} relative to the separated reactants as listed in **Table 2**. As shown in **Figure 3**, the sulfur atom of SCP holds large positive charge (2.326), it indicates that sulfur is the most electrophilic atom of sulfonyl group. With the oxygen atom O1 of the nucleophilic water molecule possessing negative charge (-1.050) attacking the sulfur atom of the electrophilic sulfonyl group, the nucleophilic substitution takes place and a transition state **TS2** was formed, the energy comes to be 48.18 kcal·mol^{-1} higher than those of the separated

Table 2. Total Energies with ZPE and Relative Energies of the hydrolysis mechanisms of neutral, once-protonated and double protonated SCP

Compounds	Total Energies with ZPE (Hartree)	Relative Energies (kcal·mol^{-1})
SCP+H_2O (path 1 in neutral from)	-1690.524866	0
Intermediate 1	-1690.527401	-1.59
TS2	-1690.448067	48.18
Product 3	-1690.534375	-5.97
SCP+ H_2O (path 2 in neutral form)	-1690.524866	0
Intermediate 4	-1690.526073	-0.26
TS5	-1690.432646	57.85
Product 6	-1690.529267	-2.76
SCP+ H_2O (path 1 in once-protonated form)	-1690.932493	0
Intermediate 7	-1690.932501	0.00
TS8	-1690.848757	52.53
Product 9	-1690.941452	-5.62
SCP+ H_2O (path 2 in once-protonated form)	-1690.932493	0
Intermediate 10	-1690.932546	-0.03
TS11	-1690.831925	63.09
Product 12	-1690.937630	-3.22
SCP+ H_2O (path 1 in double-protonated form)	-1691.342814	0
Intermediate 13	-1691.356691	-8.71
TS14	-1691.278832	48.84
Product 15	-1691.369689	-8.15
SCP+ H_2O (path 2 in double-protonated form)	-1691.342814	0
Intermediate 16	-1691.356595	-8.65
TS17	-1691.254910	63.79
Product 18	-1691.349971	4.16

reactants as summarized in **Table 2**. With the old bonds S-N and O1-H breaking and new bonds O1-S and N-H forming, the products **3** sulfanilic acid and 6-chloro-3-pyridazinamine were produced as depicted in **Figure 3**. As listed in **Table 3**, the energy barrier was estimated to be 49.77 kcal·mol^{-1} for the hydrolysis pathway 1.

The second pathway of SCP hydrolysis resembles an aromatic nucleophilic substitution, which occurs in a way of water molecule attacking the electrophilic heterocyclic aromatic group, where the sulfanilamide and 3-Chloro-6-pyridazone molecules are the products. The hydrolysis reaction starts by forming the stable intermediate **4** (**Figure 4**) with the hydrogen bond O1-H…N(2.12Å) as given in **Figure 4**, which results in the energy of intermediate **4** slightly decreased by 0.26 kcal·mol^{-1} compared to the separated reactants as illustrated in **Table 1**. As shown in **Figure 4**, the calculated NBO charge indicates that of C atom in the heterocyclic aromatic ring carries positive charge acting as an electrophile. Consequently, the electrophilic C atom is attacked by the water molecule to give the unstable transition state **TS5** (**Figure 4**) with an energy of 57.85 kcal·mol^{-1} relative to the separated reactants as listed in **Table 2**. With the H atom of water molecule transferring to the sulfonyl group, the hydroxyl group to the C atom of the heterocyclic aromatic ring, eventually the products **6** (sulfanilamide and 3-Chloro-6-pyridazone) were obtained, the corresponding energy was -2.76 kcal·mol^{-1} relative to the separated reactants. The energy barrier of 58.11 kcal·mol^{-1} was predicted for the second hydrolysis pathway of neutral SCP. All the energy barriers of the two pathways were summarized in **Table 3**. **Figure 5** illustrated the relative energy profile

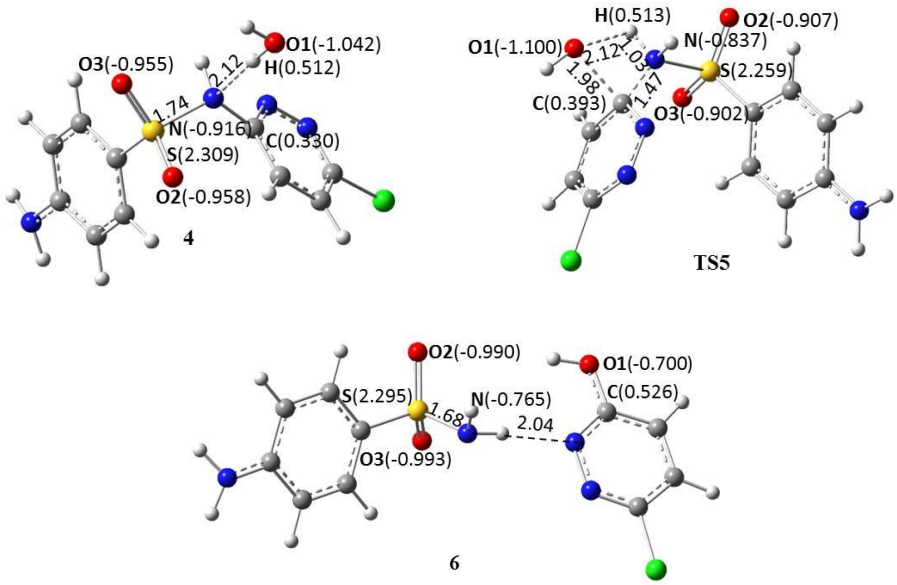

Figure 4: Optimized structures of intermediate **4**, transition state **TS5** and product **6** for the pathway 2 of neutral SCP hydrolysis mechanism.

of the two hydrolysis pathways of neutral SCP. Hydrolysis pathway 1 and 2 both are typical nucleophilic substitutions attacked by water molecule, which occur in the sulfonyl group and the heterocyclic aromatic ring respectively. In comparison, the electrophilic center sulfur carries a positive charge of 2.326 as labeled in **Figure 3** (1), which is much larger than that of carbon atom C1 (0.330) in the heterocyclic aromatic ring, which may cause the sulfur atom can be more easily attacked by water molecule, and pathway 1 is more energetically favorable than pathway 2, which is in a good accordance with the experimental investigations obtained from HPLC analyses, where much more hydrolysis product sulfanilic acid were observed than that of the sulfanilamide in the SCP hydrolysis at 70˚C [4].

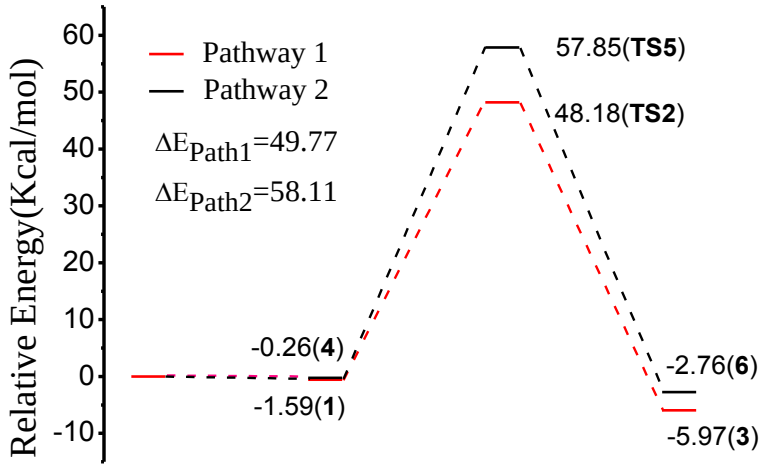

Figure 5: The relative energy profile of two hydrolysis mechanism pathways for neutral SCP

Table 3. Energy barriers for the hydrolysis mechanisms of neutral, once-protonated and double protonated SCP

Hydrolysis Mechanism Reactions	Energy Barrier (kcal·mol^{-1})
Neutral SCP(a)+ H_2O	
pathway 1	49.77
pathway 2	58.11
Once-protonated SCP(b)+ H_2O	
pathway 1	52.54
pathway 2	63.12
Double-protonated SCP(c)+ H_2O	
pathway 1	57.55
pathway 2	72.44

3.2 Hydrolysis mechanisms of once-protonated SCP

If the pH of solution less than the pK_{a2}=2.2, SCP is predominantly present in once-protonated form SCP (II) as displayed in **Figure 1**. As discussed in the hydrolysis mechanisms of neutral SCP, two similar hydrolysis pathways were postulated as shown in **Scheme 1**. **Figure 6** illustrates the optimal geometries of the stable intermediate **7**, transition state **TS8**, and product **9** for the once-protonated SCP hydrolysis pathway 1. Firstly the stable intermediate **7** was formed with a weak hydrogen bond namely O1-H…N (2.19Å) between SCP and H_2O as shown in **Figure 6**, the total energy was slightly lowered relative to the separate reactants. With the reaction proceeding, the O1 of water molecule approaches to the most electrophilic sulfur atom of the sulphonyl group, the transition state **TS8** (**Figure 6**) with a strained four membered ring was obtained as shown in **Figure 6**. Finally, with the old bonds S-N and O1-H breaking and the new bonds O1-S and H-N forming, the products **9** (**Figure 6**) were yielded. For the once-protonated SCP hydrolysis pathway 1, the energy barrier of 52.54 kcal·mol^{-1} was estimated as listed in **Table 3**.

The once-protonated SCP can also be hydrolyzed by the second pathway as displayed in **Scheme 1**. In the pathway 2, the stable intermediate **10** was firstly obtained with hydrogen bonding O1-H…N (2.19Å) as shown in **Figure 7**. The nucleophilic substitution takes place by

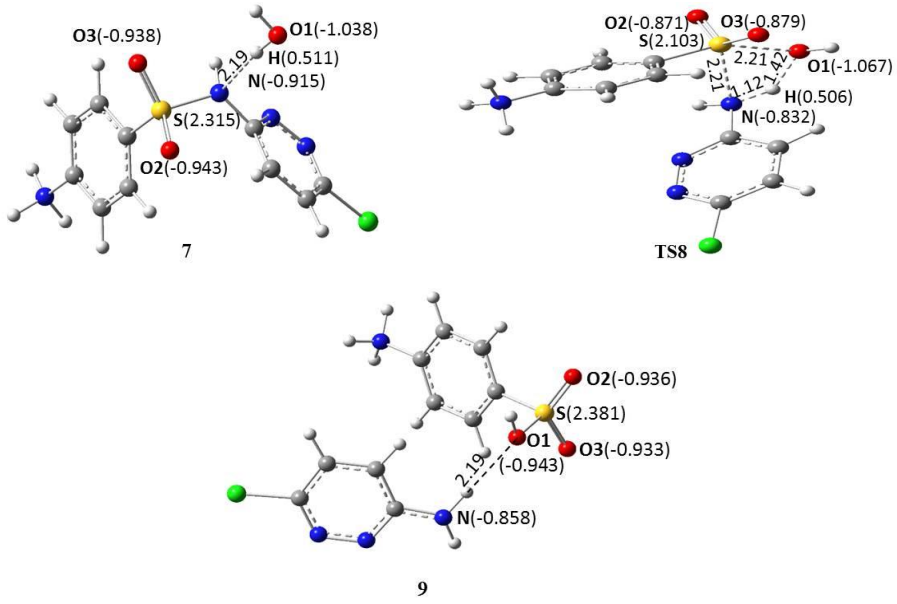

Figure 6: Optimized structures of intermediate **7**, transition state **TS8** and product **9** for the pathway 1 of once-protonated SCP hydrolysis mechanism.

the water molecule attacking on the electrophilic carbon atom C with a positive charge (0.324) in heterocyclic aromatic group instead of the sulfonyl group, the transition state **TS11** characterized by a high strained four-member ring were then generated with the energy of 63.09 kcal·mol^{-1} (**Table 2**) much higher in comparison with the separated reactants. With H transferring from water molecule to N of the sulfonyl group and the hydroxyl group to heterocyclic ring, the new N-H and C-O1 bonds formed and the final products **12** were obtained as shown in **Figure 7**. In comparison with the energy of pre-complex intermediate **10**, the energy barrier of 63.12 kcal·mol^{-1} was obtained.

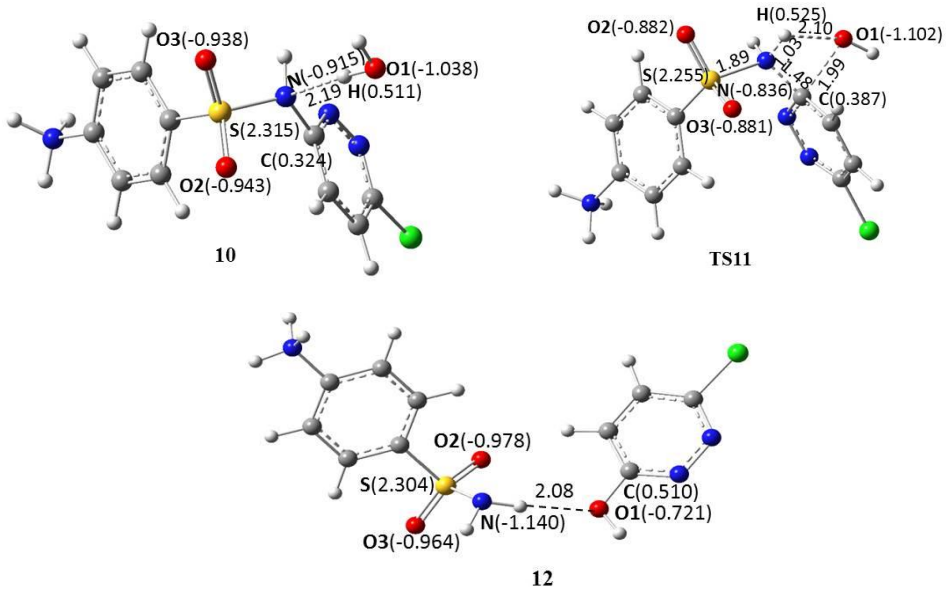

Figure 7: Optimized structures of intermediate **10**, transition state **TS11** and product **12** for the pathway 2 of once-protonated SCP hydrolysis mechanism.

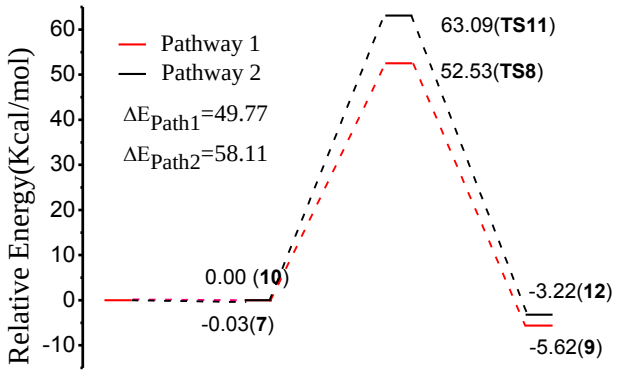

Figure 8: The relative energy profile of two hydrolysis mechanism pathways for once-protonated SCP.

The relative energy profile of two hydrolysis mechanism pathways was presented in **Figure 8** for once-protonated SCP. As in the case of the neutral SCP hydrolysis, the electrophilic sulfur (2.315) of sulfonyl group carries much larger positive charge that of carbon atom C (0.324) in the heterocyclic aromatic ring, the sulfur atom can react easily with water molecule, which may lead to the pathway 1 holds a considerable lower energy barrier than the pathway 2 (52.54 kcal·mol^{-1} < 63.12 kcal·mol^{-1}).

3.3 Hydrolysis mechanisms of double protonated SCP

Due to the very low pK_{a1}(<2), the double protonated SCP can only exist under very acidic conditions as shown in **Figure 1**. As presented in the neutral and once-protonated SCP hydrolysis, two independent hydrolysis mechanisms were suggested for the double protonated SCP. In the first pathway, the stable intermediate **13** was first obtained with strong hydrogen bonds N-H1…O1 (1.90Å) and N-H2…O1 (1.86Å) between the double protonated SCP and water molecule as illustrated in **Figure 9**, which results in the total energy was hugely lowered by 8.71 kcal·mol^{-1} relative to the separated reactants as indicated in **Table 2**. As shown in **Figure 9**, with the O1 of water molecule interacting with the electrophilic sulfur atom, the hydrolysis reaction follows a nucleophilic substitution process to give a transition state **TS14** with the energy 48.84 kcal·mol^{-1} high above the separated reactants. Thereafter, the products **15** were achieved with the S-N, O1-H bonds breaking and new S-O1, H-N bonds forming. **Table 2** summarized the total energies of the intermediate **13**, transition state **TS14** and products **15.** Due to the very stable pre-complex structure **13** with

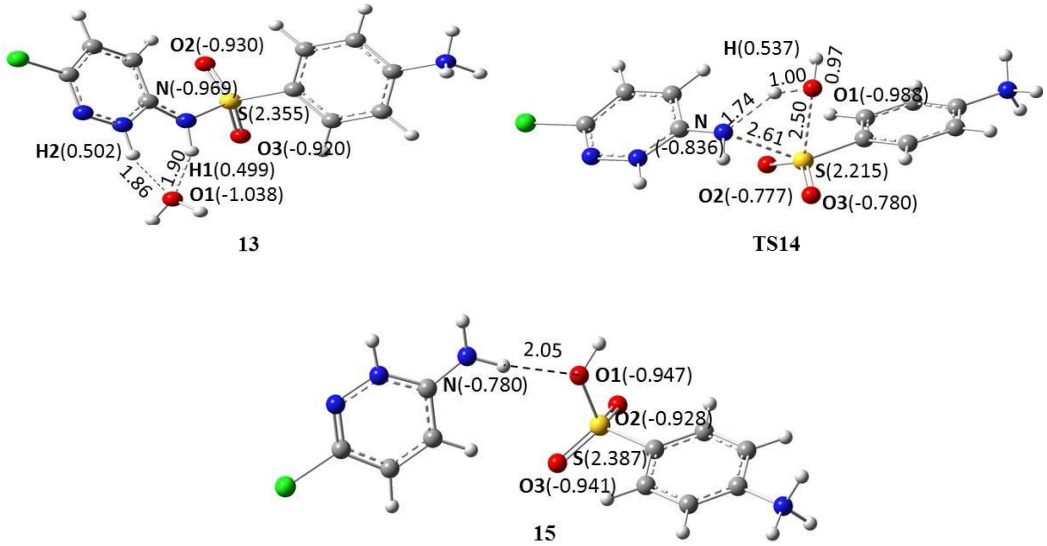

Figure 9: Optimized structures of intermediate **13**, transition state **TS14** and product **15** for the pathway 1 of double-protonated SCP hydrolysis mechanism.

the low energy of -8.71 kcal·mol^{-1}, the energy barrier is estimated to be 57.55 kcal·mol^{-1}, which is much higher than those of neutral and once-protonated SCP as illustrated in **Table 3**.

In the initial stage of pathway 2, the hydrogen bonds N-H1…O1 (1.85Å) and N-H2…O1 (1.91Å) was formed between the SCP and water as shown in **Figure 10**, which leads to the pre-complex **16** with the energy of -8.65 kcal·mol^{-1} significantly lower than the separate reactants as given in **Table 2**. Attacking on the electrophilic C (0.459) heterocyclic ring by the water molecule leads to the unstable transition state **TS17** (**Figure 10**) with the corresponding energy of 63.79 kcal·mol^{-1} (**Table 2**) relative to the respective reactants as given in **Table 2**. Finally, the products **18** were yielded with the old bonds of O1-H and N-C breaking. Due to the stable pre-complex structure **16** with much low energy, the high energy barrier of 72.44 kcal·mol^{-1} was obtained as listed in **Table 3**. **Figure 11** depicts the relative energy profile of the hydrolysis mechanism pathways for double protonated SCP. Similar to the hydrolysis mechanism of neutral and once-protonated SCP, the electrophilic sulfur (2.355) of sulfonyl group has much larger positive charge than that of carbon atom C (0.459) in the heterocyclic aromatic ring, the sulfur atom can be more easily attacked by water molecule, which causes that pathway 1 is more energetically favorable than pathway 2 for the double protonated SCP hydrolysis.

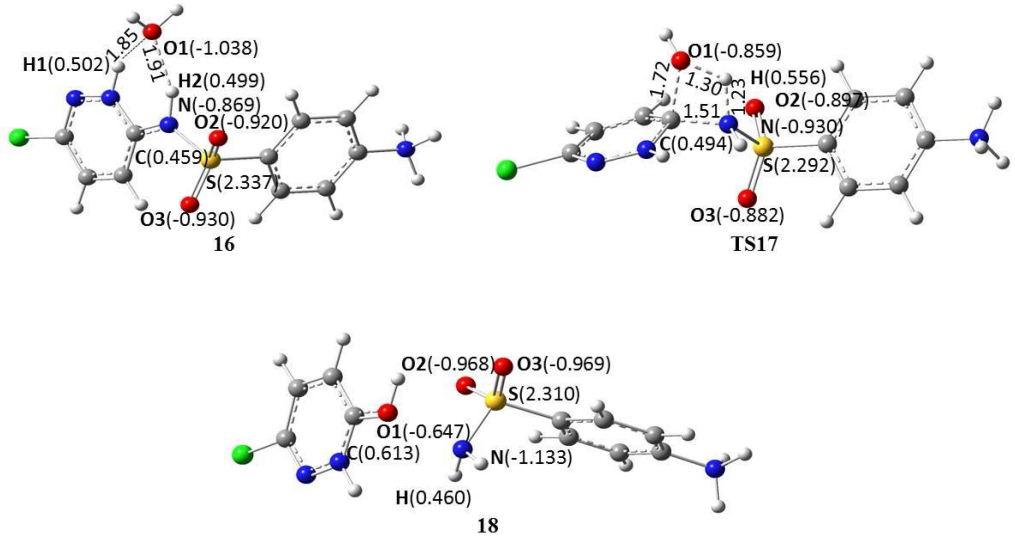

Figure 10: Optimized structures of intermediate **16**, transition state **TS17** and product **18** for the pathway 2 of double protonated SCP hydrolysis mechanism.

As summarized in **Table 3**, the comparison of two pathways shows that the pathway 1 with lower energy barrier can be the main path for the SCP hydrolysis, which may result

from the electrophilic center sulfur carrying much larger positive charge than the carbon atom in the heterocyclic aromatic ring, the sulfonyl group can be easily attacked by water molecule. As forming the stable pre-reactant complexes, the hydrolysis of double protonated SCP has much higher energy barrier than that of neutral and once protonated form. By comparing the hydrolysis energy barrier of neutral SCP with once protonated and double protonated SCP, it is obvious that the neutral SCP hydrolysis is most energetically favorable. Due to the strong repulsion between the anionic SCP and water, the hydrolysis may not take place, the hydrolysis path was not found by the density function theory. When the pH=9 in solution much large than pK_{a3}=5.5, the SCP primary exists in anionic state SCP (IV), the hydrolysis rate is relatively low. However, under weak acidic conditions pH<pK_{a3}, the decrease of pH causes the neutral and cationic forms of SCP increase, which leads to the increase of hydrolysis rate. In particular, at pH≈(pK_{a2}+pK_{a3})/2=3.85, the neutral SCP is predominant. Therefore, the hydrolysis process is much favorable. These results are in accordance with the HPLC analyses by Kumirska that the hydrolysis rate at pH=4.0 is highest in comparison with pH=7.0 and 9.0[4].

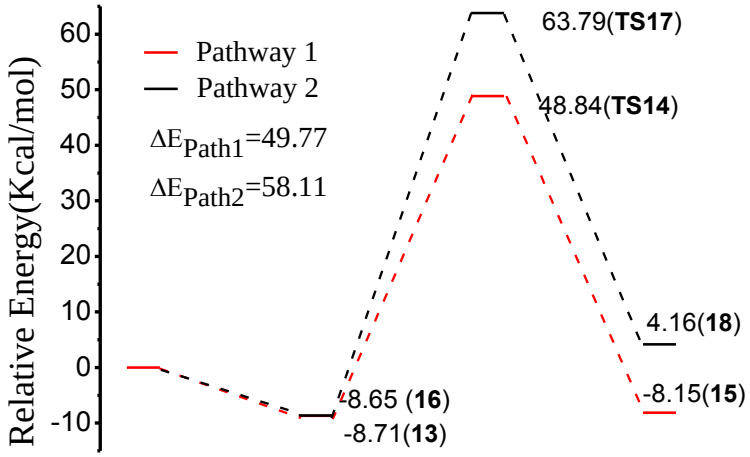

Figure 11: The relative energy profile of two hydrolysis mechanism pathways for double protonated SCP.

4 Conclusions

To understand the hydrolysis behavior of sulfonamides, two independent hydrolysis mechanisms pathways of sulfachloropyridazine in neutral, once-protonated, double protonated and dissociated anionic forms were investigated by using the density functional theory at the B3LYP/6-31+G (d, p) level. Owing to the strong repulsion between the anionic SCP and water molecule, the hydrolysis of anionic SCP hardly take place. Based on the computed energy barriers, the hydrolysis of neutral and once-protonated SCP are much more energetically favorable to proceed than those of the double protonated form. At

pH≈(pK_{a2}+pK_{a3})/2=3.85, the neutral SCP is the principal species, the hydrolysis process is relatively fast, which is in a good agreement with the HPLC analyses by Kumirska that the hydrolysis rate at pH=4.0 is highest in comparison with pH=7.0 and 9.0. As the electrophilic sulfur of sulfonyl group carries much larger positive charge than that of carbon atom C in the heterocyclic aromatic ring, the sulfur atom can be more easily attacked by water molecule, which causes the nucleophilic substitution taking place on the sulfonyl group (path 1) can be the main hydrolysis pathway.

5 Acknowledge

This work was supported by the Project of Shenzhen Science and Technology (JCYJ20160520162818982) and National Science Foundation of China-Guangdong Provincial People's Government jointly fund and National Supercomputing Center in Guangzhou.

References

[1] M. J. García-Galán, M. S. Díaz-Cruz, D. Barceló, Identification and determination of metabolites and degradation products of sulfonamide antibiotics, TrAC Trends in Analytical Chemistry, 27 (2008), 1008-1022.

[2] M. J. García-Galán, M. S. Díaz-Cruz, D. Barceló, Combining chemical analysis and ecotoxicity to determine environmental exposure and to assess risk from sulfonamides, TrAC Trends in Analytical Chemistry, 28 (2009), 804-819.

[3] K.-R. Kim, G. Owens, S.-I. Kwon, K.-H. So, D.-B. Lee, Y. S. Ok, Occurrence and Environmental Fate of Veterinary Antibiotics in the Terrestrial Environment, Water Air and Soil Pollution, 214 (2011), 163-174.

[4] A. Białk-Bielińska, S. Stolte, M. Matzke, A. Fabiańska, J. Maszkowska, M. Kołodziejska, B. Liberek, P. Stepnowski, J. Kumirska, Hydrolysis of sulphonamides in aqueous solutions, Journal of hazardous materials, 221 (2012), 264-274.

[5] A. K. Bialk-Bielinska, J; Stepnowski, P., in: M. Nageeb Rashed (Ed.), Organic Pollutants-Monitoring, Risk and Treatment InTech, Rijeka, Croatia,59-86 (2013).

[6] W. Baran, E. Adamek, J. Ziemiańska, A. Sobczak, Effects of the presence of sulfonamides in the environment and their influence on human health, Journal of hazardous materials, 196 (2011), 1-15.

[7] A. Göbel, A. Thomsen, C. S. McArdell, A. Joss, W. Giger, Occurrence and sorption behavior of sulfonamides, macrolides, and trimethoprim in activated sludge treatment, Environmental science & technology, 39 (2005), 3981-3989.

[8] A. Białk-Bielińska, S. Stolte, J. Arning, U. Uebers, A. Böschen, P. Stepnowski, M. Matzke, Ecotoxicity evaluation of selected sulfonamides, Chemosphere, 85 (2011), 928-933.

[9] D. M. Blake, Bibliography of work on the heterogeneous photocatalytic removal of hazardous compounds from water and air, National Renewable Energy Laboratory, 1994.

[10] L. Hu, P. M. Flanders, P. L. Miller, T. J. Strathmann, Oxidation of sulfamethoxazole and related antimicrobial agents by TiO 2 photocatalysis, Water Research, 41 (2007), 2612-2626.

[11] S. Shah, H. M. Zhang, X. D. Song, C. Hao, Quantum chemical study of the photolysis mechanisms of sulfachloropyridazine and the influence of selected divalent metal ions, Chemosphere, 138 (2015), 765-769.

[12] S. Wang, X. D. Song, C. Hao, Z. X. Gao, J. W. Chen, J. S. Qiu, Elucidating triplet-sensitized photolysis mechanisms of sulfadiazine and metal ions effects by quantum chemical calculations, Chemosphere, 122 (2015), 62-69.

[13] J. Klimes, M. Mokry, TLC detection of photolytic and hydrolytic degradation products of selected antibacterial sulfonamides, Jpc-Journal of Planar Chromatography-Modern Tlc, 9 (1996), 61-64.

[14] M. J. Frisch, G. Trucks, H. Schlegel, G. Scuseria, M. Robb, J. Cheeseman, G. Scalmani, V. Barone, B. Mennucci, G. Petersson, Gaussian 09, revision C. 01, Gaussian Inc., Wallingford, CT, 2010.

[15] D. Zhao, P. Feng, K. Han, X. Chen, A theoretical investigation of the adsorption activity of dnl-6 by dft method, Commun Comput Chem, 3 (2015), 11-17.

[16] S. Sun, P. Song, F. Ma, A DFT/TDDFT investigation on the ESIPT mechanism of a novel sensor BIP, Commun. Comput. Chem, 4 (2016), 9-23.

[17] Z. Wen, W. Hu, X. Chi, X. Wang, D. Tian, M. Wang, J. Liu, X. Ma, A. Pang, DFT Study of the catalytic mechanism for urethane formation in the presence of basic catalyst 1, 4-diazabicyclo [2.2. 2] octane, Commun Comput Chem, 2 (2014), 22-35.

[18] H. Li, H. Yin, X. C. Liu, Y. Shi, TDDFT assessment of excited state intramolecular proton transfer in a panel of chromophore 2-hydroxypyrene-1-carbaldehyde, Journal of Atomic and Molecular Sciences, 7 (2016), 115-124.

[19] C. Lv, L. Sun, B. Wang, C. Zhang, J. Zhang, A TDDFT Study on Fluorescent Chemosensor for Fluoride Anion Based on Dipyrrolyl Derivatives, Commun. Comput. Chem, 1 (2013), 282-296.

[20] D. Li, Y. Wang, K. Han, Recent density functional theory model calculations of drug metabolism by cytochrome P450, Coordination Chemistry Reviews, 256 (2012), 1137-1150.

[21] Z. Lou, P. Li, K. Han, Redox-Responsive Fluorescent Probes with Different Design Strategies, Accounts of Chemical Research, 48 (2015), 1358-1368.

[22] A. D. Becke, DENSITY-FUNCTIONAL THERMOCHEMISTRY .3. THE ROLE OF EXACT EXCHANGE, Journal of Chemical Physics, 98 (1993), 5648-5652.

[23] A. d. Becke, Becke's 3 parameter functional combined with the non-local correlation LYP J, Chem. Phys, 98 (1993), 5648.

[24] C. Lee, W. Yang, R. G. Parr, Development of the Colle-Salvetti correlation-energy formula into a functional of the electron density, Physical review B, 37 (1988), 785.

[25] C. A. Leverett, V. C. Purohit, A. G. Johnson, R. L. Davis, D. J. Tantillo, D. Romo, Dyotropic Rearrangements of Fused Tricyclic beta-Lactones: Application to the Synthesis of (-)-Curcumanolide A and (-)-Curcumalactone, Journal of the American Chemical Society, 134 (2012), 13348-13356.

[26] Y. Yuan, W. Hu, X. H. Chi, C. H. Li, D. Y. Gui, M. L. Wang, J. H. Liu, X. G. Ma, A. Pang, First principle simulation on oxidation mechanism of diethyl ether by nitrogen dioxide, Journal of Theoretical & Computational Chemistry, 14 (2015), 1550020.

[27] J. P. Cao, Y. L. Liu, A. J. Shi, Y. Yuan, M. L. Wang, A DFT study on the mechanism of reaction between 2, 4-diisocyanatotolune and cellulose, Journal of Theoretical & Computational Chemistry, 15 (2016), 1650012.

[28] Y. Yuan, J. P. Cao, Y. L. Liu, A. J. Shi, Q. Zhang, X. X. Lin, M. L. Wang, Catalytic Effects of Water Clusters on the Hydrolysis of Toluene-2,4-diisocyanate: A DFT Study, Bulletin of the Chemical Society of Japan, 89 (2016), 74-91.

[29] M. Cossi, V. Barone, R. Cammi, J. Tomasi, Ab initio study of solvated molecules: a new implementation of the polarizable continuum model, Chemical Physics Letters, 255 (1996), 327-335.

[30] E. Cances, B. Mennucci, J. Tomasi, A new integral equation formalism for the polarizable continuum model: Theoretical background and applications to isotropic and anisotropic dielectrics, The Journal of chemical physics, 107 (1997), 3032-3041.

[31] D. G. Truhlar, B. C. Garrett, Variational transition state theory, Annual Review of Physical Chemistry, 35 (1984), 159-189.

[32] D. G. Truhlar, B. C. Garrett, S. J. Klippenstein, Current status of transition-state theory, The Journal of physical chemistry, 100 (1996), 12771-12800.

[33] K. J. Laidler, M. C. King, Development of transition-state theory, The Journal of physical chemistry, 87 (1983), 2657-2664.

[34] M. Cossi, N. Rega, G. Scalmani, V. Barone, Energies, structures, and electronic properties of molecules in solution with the C-PCM solvation model, Journal of computational chemistry, 24 (2003), 669-681.

[35] K. Kim, G. Frenking, C. Dykstra, C. E. Dykstra, Theory and Applications of Computational Chemistry: The First Forty Years, Elsevier Science Limited, 2005.

[36] X. X. Wang, W. Hu, D. Y. Gui, X. H. Chi, M. L. Wang, D. Y. Tian, J. H. Liu, X. G. Ma, A. M. Pang, DFT Study of the Proton Transfer in the Urethane Formation between 2,4-Diisocyanatotoluene and Methanol, Bulletin of the Chemical Society of Japan, 86 (2013), 255-265.

[37] A. E. Reed, R. B. Weinstock, F. Weinhold, Natural population analysis, The Journal of Chemical Physics, 83 (1985), 735-746.

[38] A. E. Reed, L. A. Curtiss, F. Weinhold, Intermolecular interactions from a natural bond orbital, donor-acceptor viewpoint, Chemical Reviews, 88 (1988), 899-926.

[39] Y. S. Tan, Z. F. Chen, L. Hong, Y. Zhang, Sulfachloropyridazine, Acta Crystallographica Section E-Structure Reports Online, 61 (2005), O1842-O1844.